Clinical and Experimental Health Sciences

Proteomic Analysis in Nifedipine Induced Gingival Overgrowth: A Pilot Study

Ece Yetis[1], Aysen Yarat[2], Onur Eroglu[1], Hafize Ozturk Ozener[3], Leyla Kuru[3]

[1] Marmara University, Institute of Health Sciences, Department of Periodontology, Istanbul, Türkiye.
[2] Marmara University, Faculty of Dentistry, Department of Basic Medical Sciences, Istanbul, Turkiye.
[3] Marmara University, Faculty of Dentistry, Department of Periodontology, Istanbul, Türkiye.

Correspondence Author: Leyla Kuru
E-mail: lkuru@marmara.edu.tr
Received: 29.12.2021 **Accepted:** 16.05.2022

ABSTRACT

Objective: The aims of the present study were to investigate the proteomic profile of nifedipine induced overgrown gingiva and compare with non-overgrown gingival tissues obtained from the same patients.

Methods: Seven subjects under nifedipine medication for at least 6 months and diagnosed as nifedipine induced gingival overgrowth (NIGO) participated in the study. Periodontal clinical parameters were recorded. Gingival tissue samples were harvested from overgrown (GO+ Group, n=7) and non-overgrown regions (GO- Group, n=7) of the same patients. Proteomics was performed using Liquid Chromatography-Tandem Mass Spectrometry (LC-MS/MS) technique. The identified proteins were further classified according to their molecular functions, biological processes and cellular component distribution for functional gene ontology analysis using a web-based bioinformatics tool. Mann Whitney-U and ANOVA tests were performed to compare clinical parameters and identified proteins with proteomics, respectively.

Results: Bleeding on probing and gingival overgrowth index of the GO+ group were statistically significantly higher than the GO- group ($p<0.05$, $p<0.01$, respectively). A total of 143 proteins were identified in 14 gingival tissue samples using proteomics. Among the proteins identified, 79 of them were detected in higher quantities in the GO+ group ($p<0.05$) whereas remaining 64 were found higher in the GO- group ($p<0.05$). The analysis of functional gene ontology demonstrated that certain proteins exhibit roles in either stimulatory or inhibitory processes including cell proliferation, growth and apoptosis.

Conclusion: The proteomic profiles of overgrown and non-overgrown gingiva suggest that the identified proteins expressed at different levels in both groups may contribute to the pathogenesis and progression of NIGO.

Keywords: gingival overgrowth, nifedipine, proteomics

1. INTRODUCTION

Gingival overgrowth (GO), a pathological clinical situation, is defined as the increase in size and the change in contour of gingiva observed as a common symptom in various gingival diseases and systemic conditions. It can be temporary and reversible or chronic and irreversible, associated with many factors such as inflammation, side effects of certain medications, and neoplastic pathologies (1). When it occurs as a side effect and an undesirable consequence of systemically used drugs, it is then called drug-induced GO (DIGO) which is limited to the gingival tissues, but not a periodontium-induced pathology. The inducing drugs are anticonvulsants, immunosuppressants and calcium channel blockers (CCBs). Worldwide used CCBs have proven to be extremely effective to take the hypertension under control. According to their chemical composition, CCBs can be classified under three main classes as benzothiazepines, phenylalkylamines and dihydropyridines (2).

The gingival changes due to the use of CCBs present similar clinical features. CCB induced GO is localized on attached gingiva and gingival margin, and visible first on interdental papillae with a lobular or nodular morphology extending through occlusal surfaces coronally and mucogingival junction apically, covering the clinical crown (3). Lesions are located mostly on the anterior vestibular surfaces whereas some regions in the same subject may not show any sign of GO. With the reach of overgrown gingiva coronally, aesthetic, functional and phonational difficulties may occur (4).

Among CCBs, nifedipine has been the most frequently used drug inducing GO with a wide prevalence ranging from 15%

DOI: 10.33808/clinexphealthsci.1050418

to 83% (5), followed by diltiazem (6) and verapamil (7) with ratios of 21% and 4%, respectively.

It is proposed that the incidence of nifedipine induced GO (NIGO) appears to increase in the next period of time, since the use of antihypertensive drugs, especially nifedipine and the indication of hypertension as a symptom of various systemic diseases such as metabolic syndrome in the society, increase. Thereby, it is of utmost importance to clarify the cellular and molecular mechanisms of NIGO.

The upregulatory process or causative molecule is still under the concern of researchers. Numerous theories and hypotheses have been speculated in the literature. Nifedipine may act indirectly by stimulating the production of interleukin-2 by T cells (8) or testosterone metabolites (9). Some changes in calcium ion metabolism may also account for GO (5). The upregulation in proliferative and synthetic activity of fibroblasts are followed by the increase in extracellular matrix (ECM) and tissue volume. In addition, transforming growth factor-ß (TGF-ß), fibroblast growth factor and heparan sulphate glycosaminoglycan play a role in NIGO (10). Angiotensin-II, which is involved in fibrosis mechanism by increasing the TGF-ß and connective tissue growth factor levels, was found to be higher in gingival samples with NIGO compared to healthy controls (11).

With the development of genomic, proteomic, or metabolomic techniques, it is now possible to define the key factors of disease pathogenesis more efficiently. Proteomics provides a great advantage on identifying potential disease markers since very low levels of proteins can be detected, and also compares the expression profile of proteins from a cell, tissue or organism with state of health and non-standard condition such as a disease or presence of a toxin in a spontaneous reference state (12). In dental field, enamel, dentin, pulp, microorganisms, stem cells and various dental materials have been successfully examined using this novel technique (13, 14). Proteomics has been also applied in periodontology to investigate dental plaque, oral mucosa, gingiva, periodontal ligament, cementum, alveolar bone, gingival crevicular fluid (GCF) and saliva (15, 13).

Until now, there is only one experimental study examining the upregulated and downregulated proteins expressed by cultured gingival fibroblasts treated with 10 µM of immunosuppressant cyclosporin-A for 48 hours using proteomics technique (16). Jung et al. reported that 17 proteins are related with cell proliferation. However so far, the exact pathogenic mechanism of NIGO has still not been clarified. Therefore, the aim of the present study was to investigate the proteomic profile of nifedipine induced overgrown gingiva, and compare with non-overgrown gingival tissues obtained from the same patients.

2. METHODS

2.1. Study Population

This cross-sectional study was approved by the Ethical Committee of Marmara Faculty of Dentistry with a protocol number of 2018-175. Written informed consent, detailing the study protocol was obtained from all participants. Seven subjects (Male/ Female (M/F), 3/4; mean age of 43.42± 15.29 years) under nifedipine medication of 30 mg per day, for at least 6 months and diagnosed with NIGO were enrolled in the study.

Inclusion criteria were: 1) having at least 12 teeth, 2) non-smoker, 3) not being pregnant, 4) not using antibiotics or anti-inflammatory drugs in the past 6 months, 5) not having periodontal treatment in the past 6 months.

2.2. Clinical Procedures

Clinical parameters including plaque index (PI) (17), gingival index (GI) (18), probing depth (PD) and bleeding on probing (BOP) were recorded by a calibrated single researcher (E.Y.) with using a 0.5 mm diameter and 15 mm periodontal probe (University of North Carolina, PCPUNC15, Hu-Friedy Ins Co, USA). In addition, GO index developed by Ellis et al. (19) was evaluated on 10 anterior papilla (13 to 23, and 33 to 43) using intraoral photographs taken from patients and projected on a screen. The calibration of the researcher was calculated by Cohen's Kappa analysis on GO index which was measured twice with 24 hours interval (κ= 0.84, $p<0.001$).

Criteria for assessing GO on adjacent tooth surfaces for a gingival unit are as follows:

0= No encroachment of interdental papilla onto tooth surface

1= Mild encroachment of interdental papilla, producing a blunted appearance to papilla tip

2= Moderate encroachment, involving lateral spread of papilla across buccal tooth surface of less than 1/3 tooth width

3= Marked encroachment of papilla, more than 1/4 tooth width. Loss of normal papilla form

Using this index, the maximum score obtainable was 30 which was then converted to a percentage GO score and recorded.

2.3. Sample Collection

Gingival tissue samples were harvested from overgrown (GO+ Group, n=7) and non-overgrown regions (GO- Group, n=7) of the same patients diagnosed with NIGO. While the GO+ group tissues were obtained by the excision for therapeutic purposes during flap operation or gingivectomy procedure, the GO- group samples were obtained during crown lengthening operation. The excised tissue samples were placed in low-binding tubes (Eppendorf, USA) containing sterile saline and stored at – 80°C prior to the experiment.

2.4. Proteomic Analysis

2.4.1. Protein Extraction from Gingival Samples

Gingival tissue samples were homogenized and pooled for each group. For protein extraction, the tissue homogenate was mixed with Universal Protein Extraction (UPX) Kit (Abcam, UK) and protease inhibitor cocktail (Abcam, UK) at a ratio of 1:100. The tissue homogenates were centrifuged at 18.000 rpm for 10 minutes. The supernatant containing soluble proteins was obtained and transferred into low-binding tubes (Eppendorf, USA). Protein concentrations in the samples were determined by the method of Biorad Bradford protocol (Bio-Rad, Hercules, USA) (20). Peptide concentration was measured by Pierce's quantitative colorimetric peptide determination method (Pierce ™ Quantitative Colorimetric Peptide Assay, Thermo Fisher Scientific, USA) (21). The samples were diluted with 0.1% formic acid so that the final concentration was 200 ng/µL.

2.4.2. Identification and Quantitative Analysis of Proteins

Following the chromatographic separation by liquid chromatography (LC), molecules were ionized. The interface used in this study was the LC-Tandem Mass Spectrometry (LC-MS/MS) method was based on electrospray ionization. Further specificity was obtained with multiple ionization events. The analyzed data were collected for peptides that could be identified in the m/z 50-2000 range. MS was performed following the electrospray ionization. MS analysis was performed for 0.5 seconds and information about the entire peptide was collected. Then, MS/MS analysis was performed for 0.5 seconds, and the peptide was fragmented and sequence information was obtained.

Protein identification was carried out using human protein sequence information in the UniProt protein database (22). Primary accession number, entry name of UniProt database and molecular weight for each identified protein were reported.

2.5. Classification of Identified Proteins

These identified proteins were further classified according to their molecular functions, biological processes and cell localization for functional gene ontology analysis using a web-based bioinformatics tool (Panther Analysis Gene Ontology Classification System, version 16.0, Panther, USA) (23).

2.6. Statistical Analysis

The analysis for clinical data was performed using the IBM SPSS, version 22.0 for Windows. Mann Whitney-U test was performed to compare clinical parameters between the groups. The analysis for proteomic data was performed by the Progenesis QIP software (Waters, USA). The ANOVA test was applied to compare the identified protein levels between the groups. A P value of <0.05 was considered statistically significant.

3. RESULTS

Clinical periodontal parameters for whole mouth and selected regions for GO+ and GO- groups are shown in Table 1. While PI, GI and PD values of both groups were similar (p>0.05), BOP and GO index of the GO+ group were statistically significantly higher than the GO- group (p<0.05, p<0.01, respectively). All of the subjects were diagnosed as periodontitis and the details were as follows: 1 patient Grade A Stage III, 2 patients Grade B Stage III, 2 patients Grade B Stage IV and 2 patients Grade C Stage IV.

Table 1. *Clinical periodontal parameters*

	Whole Mouth n=7	GO+ Group n=7	GO- Group n=7	P*
PI	2.31±0.48	2.41±0.44	2.15±0.55	0.318
GI	1.70±0.26	1.89±0.47	1.51±0.27	0.097
PD (mm)	4.29±1.36	4.61±1.58	3.68±1.61	0.209
BOP (%)	59.42±22.81	70.17±32.98	37.90±20.60	0.038
GOI (%)	66.67±18.95	66.67±18.95	0	0.001

** Mann Whitney-U Test, p<0.05, PI: Plaque Index, GI: Gingival Index, PD: Probing Depth, BOP: Bleeding on Probing, GOI: Gingival Overgrowth Index*

A total of 143 proteins were identified in 14 gingival tissue samples using LC-MS/MS method, as shown in Table 2. The collective data revealed that among the total number of human proteins identified, 79 of them were detected in higher quantities in the GO+ group (p<0.05) whereas remaining 64 were found higher in the GO- group (p<0.05).

As shown in Figure 1, the molecular functions of the identified proteins in the GO+ group were associated with catalytic activity (53.8%), binding (38.5%), molecular function regulator (3.8%), structural molecule activity (1.9%) and transporter activity (1.9%), while the distribution of the identified proteins in the GO- group were related with, catalytic activity (33.3%), binding (48.9%), molecular function regulator (4.4%), structural molecule activity (4.4%), molecular adaptor activity (4.4%), and transporter activity (4.4%). The most up-regulated proteins in the GO+ group were found to be related with catalytic activity, whereas the proteins having a role in binding to cell surface receptors were noticed at the highest rate in the GO- group.

Figure 2 shows the distribution of identified proteins involved in biological processes for the GO+ group were as follows, cellular process (30.2%), metabolic process (22.2%), biological regulation (12.7%), response to stimulus (10.3%), localization (9.5%), signaling (4.8%), immune system process (4%), interspecies interaction between organisms (3.2%), developmental process (1.6%), multicellular organismal process (0.8%) and biological adhesion (0.8%); while the distribution for the GO- group were cellular process (30.9%), metabolic process (14.4%), localization (11.3%), biological regulation (11.3%), response to stimulus (9.3%), signaling (6.2%), developmental process (4.1%), biological adhesion (4.1%), multicellular organismal process (3.1%), immune system process (2.1%), interspecies interaction between

organisms (1%), locomotion (1%) and growth (1%). Regarding the biological processes, proteins taking role in cellular process were found to be the most markedly up-regulated proteins in both groups.

Further examination of functional and biological characteristics revealed that some of the identified proteins having roles in stimulatory or inhibitory processes may be associated with NIGO. These are; pyruvate dehydrogenase kinase isozyme 1, macrophage migration inhibitory factor, striatin, myeloid-derived growth factor, derlin, thioredoxin domain containing protein 17, annexin, peroxiredoxin-4, dolichyl-diphosphooligosaccharide-protein glycosyltransferase subunit 2, guanine nucleotide-binding protein subunit beta-1, integrin-linked protein kinase, CDKN2A-interacting protein and programmed cell death protein.

As shown in Figure 3, the cellular component distribution of proteins were classified as; cellular anatomical entity, protein containing complexes and intracellular proteins in both groups which were rated as 45.7%, 19% and 35.2% for the GO+ group, respectively; and 48.6%, 17.1% and 34.3% for the GO- group, respectively. The proteins which have cellular anatomical entity demonstrated the most elevated levels in both groups.

Table 2. *The list of identified proteins*

Protein Name	Accession Number	P Value	Q Value	Fold Change	Power
Small nuclear ribonucleoprotein	P62314	0.0494506	0.3444506	2.74500693	0.68099941
Zinc finger protein 700	Q9H0M5	0.0478779	0.3125406	4.72471546	0.795083946
Macrophage migration inhibitory factor	P34884	0.0469577	0.3905696	1.76736934	0.587594274
Coiled-coil-helix-coiled-coil-helix domain-containing protein 2	Q9Y6H1;Q5T1J5	0.0465955	0.3943175	1.77652293	0.57250119
Transcobalamin-2	Q9R0D6	0.0463088	0.2726492	4.7581034	0.861144554
S-adenosylmethionine synthase	Q4L7C7	0.0460559	0.3964464	1.7423305	0.555635061
Ankyrin repeat domain-containing protein 22	Q5VYY1	0.0460435	0.2270366	16.0487573	0.934527505
Platelet-activating factor acetylhydrolase IB subunit beta	P68402	0.045364	0.3284671	1.743945	0.700942142
Protein S100-A2	P29034	0.0437645	0.2000892	29.0562674	0.986536066
OCIA domain-containing protein 1	Q6NYD7	0.0436608	0.2479149	3.15127175	0.906039036
Pyruvate dehydrogenase (acetyl-transferring)] kinase isozyme 1	Q15118;Q63065	0.0429072	0.1410083	12.639472	0.999123168
39S Ribosomal rotein L41_ mitochondrial	Q8IXM3	0.0418746	0.3255255	9.76112542	0.711532306
Myristoylated alanine-rich C-kinase substrate	P29966	0.0418546	0.3223091	1.73490353	0.76171896
Atypical kinase COQ8A	Q60936	0.0413078	0.3943175	3.04513551	0.573975836
CDKN2A-interacting protein	Q9NXV6	0.040622	0.2135866	2.13707375	0.976937958
Dynein light chain roadblock-type 1	Q9NP97;Q8TF09	0.0401211	0.2261721	2.24604037	0.960450498
Sterol-4-alpha-carboxylate 3-dehydrogenase decarboxylating	Q15738	0.0382684	0.3943175	1.61296849	0.573906578
Minor histocompatibility antigen H13	Q8TCT9	0.0373349	0.2323764	1.85436527	0.922115453
Orotidine 5'-phosphate decarboxylase	A8Z6D0	0.0360385	0.2543735	2.44554601	0.89727168
Retroviral-like aspartic protease 1	Q53RT3	0.0354336	0.2261721	11.1586553	0.961766064
Inhibitor of Bruton tyrosine kinase	Q9P2D0	0.0345971	0.3123982	2.75312185	0.802580257
Striatin	O43815	0.0345886	0.3223091	1.67677781	0.750769371
Phosphomethylpyrimidine synthase	Q4JVZ0	0.0345613	0.3964464	1.53558654	0.563943207
Myotubularin	Q13496;Q9Z2C5	0.0344052	0.3887715	10.6141569	0.592047309
Surfeit locus protein 4	O15260	0.0337239	0.1230189	1.72952404	0.999940605
Myeloid-derived growth factor	Q969H8;Q9CPT4;P62248	0.0333449	0.277251	1.93441014	0.844173717
Grancalcin	P28676	0.033282	0.2543735	1.86803851	0.897186983
Signal recognition particle 54 kDa protein	P61011	0.0330232	0.3905696	1.52457041	0.586986556
Peptidyl-prolyl cis-trans isomerase FKBP11	Q9NYL4	0.032833	0.3223091	1.93834411	0.739459546
Programmed cell death protein 4	Q53EL6	0.0279365	0.1811616	1.70692707	0.994490283
Leucine-rich repeat-containing protein 59	Q96AG4	0.027685	0.3255255	2.37681336	0.728506738

Table 2. *The list of identified proteins (continued)*

Protein Name	Accession Number	P Value	Q Value	Fold Change	Power
Dihydrolipoyllysine-residue acetyltransferase component of pyruvate dehydrogenase complex	P10515	0.0271859	0.3943175	1.72991847	0.577789621
Gag-Pro-Pol polyprotein	P03361	0.0266269	0.3223091	5.55732404	0.740907027
Signal peptidase complex catalytic subunit SEC11C	Q9BY50	0.0265996	0.3223091	2.03108407	0.745842721
Signal peptidase complex subunit 3	P61009	0.0265591	0.2726492	1.5691254	0.853652628
Thioredoxin domain-containing protein 17	Q9BRA2	0.0264845	0.2261721	1.60326151	0.958475264
Proliferating cell nuclear antigen	Q9DEA3	0.0264741	0.3656748	18.4921742	0.621154602
S-adenosylmethionine synthase	Q9ZMN5	0.0263273	0.3444506	2.39962297	0.647887343
Annexin A3	P12429	0.0261257	0.3255255	1.79484398	0.711440398
Succinate-CoA ligase [ADP-forming] subunit beta	Q2GEF1	0.025605	0.2046882	3.70168551	0.983097635
DnaJ homolog subfamily B member 11	Q9UBS4	0.025593	0.2270366	1.53692691	0.92866995
Mesencephalic astrocyte-derived neurotrophic factor	P55145	0.0247768	0.2135866	1.77713195	0.975413303
Extracellular superoxide dismutase [Cu-Zn]	P08294	0.0247699	0.3284671	1.73638144	0.697792648
Spondin-1	Q9HCB6;Q9GLX9	0.0246131	0.3284671	1.69274015	0.70526491
Very-long-chain enoyl-CoA reductase	Q9NZ01	0.0243144	0.3255255	2.07954226	0.727043325
Dolichol-phosphate mannosyltransferase subunit 1	O60762	0.0234614	0.3444506	1.67444642	0.646561629
Aldo-keto reductase family 1 member B15	C9JRZ8	0.0233771	0.3284671	6.12802928	0.698785084
Translocon-associated protein subunit alpha	P43307	0.0233119	0.1811616	1.59502778	0.992895743
Mitochondrial 2-oxoglutarate/malate carrier protein	Q02978	0.0232578	0.1811616	1.86519549	0.993412988
Lysozyme C	P61626	0.0230058	0.3223091	2.66994427	0.740274942
Ras-related protein Rab-3C	Q96E17	0.022807	0.3444506	7.97927353	0.667355132
Glycogen phosphorylase muscle form	P11217	0.0223101	0.1410083	2.1824605	0.999180605
Putative HLA class I histocompatibility antigen alpha chain H	P01893	0.0221405	0.3444506	2.10721218	0.658071653
ATP synthase subunit alpha	Q2GER5	0.0216382	0.3223091	1.51863186	0.74143263
Marginal zone B – and B1-cell-specific protein	Q8WU39	0.0212303	0.1261953	2.41340595	0.999857756
Fumarate hydratase_ mitochondrial	P97807	0.0211739	0.3125406	3.70671211	0.787282188
Endoplasmic reticulum resident protein 29	P30040;P81623	0.0202626	0.1261953	1.64950507	0.999833658
ADP-ribosylation factor-like protein 8A	Q96BM9	0.0201756	0.3483712	2.05341452	0.63628478
Phosphoglycerate kinase 2	P09041	0.0197738	0.3588169	1.78912135	0.627392388
N-acetyl-D-glucosamine kinase	Q9QZ08	0.0191735	0.2885533	3.0009926	0.82026268
Signal peptidase complex subunit 2	Q15005	0.0188479	0.0930501	2.12728597	0.999999925
Nucleobindin-1	Q02818	0.0188328	0.3255255	1.9367718	0.719351807
Olfactomedin-like protein 1	Q6UWY5	0.0186546	0.2881296	1.86819209	0.828938891
Erythrocyte band 7 integral membrane protein	P27105	0.0181331	0.2316996	1.60684163	0.924409994
Nidogen-1	P14543	0.0174738	0.2261721	2.72995478	0.953511525
Methylmalonate-semialdehyde dehydrogenase [acylating]	Q02252	0.0159665	0.3223091	2.64178933	0.752466404
Guanine nucleotide-binding protein G(i) subunit alpha	P08754;P08753	0.0158337	0.3444506	1.98163028	0.667244381
Protein-glutamine gamma-glutamyltransferase K	P22735	0.0158215	0.3255255	2.53768358	0.710419009
Galectin-3	P17931	0.0155269	0.3444506	1.75854584	0.659501018
Eukaryotic translation initiation factor 6	O55135;P56537	0.0152499	0.3444506	2.32651092	0.655670144
Olfactomedin-like protein 3	Q9NRN5	0.0143952	0.2270366	1.71008181	0.940712533
26S proteasome regulatory subunit 4	Q90732;P46466	0.0141739	0.2000892	1.95399027	0.98548403
Leukocyte elastase inhibitor	P30740	0.014025	0.2783066	1.62640482	0.839515115
Peroxiredoxin-4	Q13162	0.0135143	0.0880851	3.13111297	0.999999996
ATP synthase subunit beta	B9E8E6	0.0132827	0.3125406	1.94261605	0.787116367
Septin-6	Q14141	0.0131362	0.1811616	2.43375325	0.993686597
Small proline-rich protein 3	Q9UBC9	0.0130156	0.1410083	4.90568906	0.99947845
Septin-14	Q6ZU15	0.0127058	0.27402	2.7950391	0.850675595
Replicase polyprotein 1ab	K9N7C7	0.0121312	0.3255255	2.07353472	0.714644895
Peripherin	P41219	0.0119551	0.2261721	2.34766417	0.953857353
Tubulin beta chain	Q7KQL5	0.0111684	0.3255255	1.71872222	0.710777958
Src substrate cortactin	Q14247	0.0109764	0.2885533	8.06699095	0.822004131
Chaperone protein DnaK	A7GXU4	0.0109734	0.3847723	3.45751798	0.601744719
Cystatin-B	P04080	0.0108682	0.3171161	1.76846961	0.772746792

Table 2. *The list of identified proteins (continued)*

Protein Name	Accession Number	P Value	Q Value	Fold Change	Power
Cartilage oligomeric matrix protein	P49747	0.0101003	0.0880851	2.47772586	0.999999996
Transmembrane protein 43	Q9BTV4	0.0100313	0.2543735	1.53673907	0.885697972
Aldehyde dehydrogenase family 3 member A2	P51648	0.0100252	0.2543735	3.32059814	0.881620602
Immunoglobulin heavy constant alpha 1	P01876	0.0093938	0.3444506	1.82173435	0.663923212
Desmin	P31001;P17661	0.0093368	0.3255255	9.10387636	0.710177479
Protein S100-A8	P05109	0.0090665	0.3255255	1.68831625	0.731313778
Biglycan	P21810	0.0087172	0.2270366	2.70289177	0.931861137
Inter-alpha-trypsin inhibitor heavy chain H1	P19827	0.0082459	0.3223091	2.53867226	0.757542475
Mimecan	P20774	0.0080826	0.113302	2.729652	0.999983623
Aldehyde dehydrogenase_ mitochondrial	P05091	0.0077833	0.241562	1.5090911	0.915501195
ATP-dependent RNA helicase eIF4A	P0CQ70;P0CQ71	0.0077791	0.3444506	2.31695327	0.66741294
Galectin-7	P47929	0.0075516	0.3125406	2.34418073	0.783540276
Catalase	P04040	0.0073611	0.277251	1.61494597	0.842294719
Heterogeneous nuclear ribonucleoprotein L	P14866	0.0069176	0.3444506	1.88765147	0.646758634
Myeloperoxidase	P05164	0.0067079	0.3444506	2.82568957	0.672256008
Hypoxia up-regulated protein 1	Q63617	0.0064996	0.3444506	1.80619151	0.677177949
Collagen alpha-2(VI) chain	Q02788	0.0059853	0.3444506	Infinity	0.671439997
Epoxide hydrolase 1	P07099	0.0059597	0.3943175	1.57980836	0.570916727
Transforming growth factor-beta-induced protein ig-h3	Q15582	0.0056148	0.3815853	1.85984727	0.606008932
Heterogeneous nuclear ribonucleoprotein R	O43390	0.0054654	0.2726492	1.53695077	0.857107301
Desmoglein-1	Q02413	0.0053651	0.3444506	1.66593836	0.65613829
Nucleoprotein TPR	P12270	0.0042724	0.3125406	3.18188131	0.789254833
Glycogen phosphorylase-brain form	P11216	0.0042699	0.3478382	1.6140184	0.64052864
Asporin	Q9BXN1	0.0041418	0.3444506	1.55111128	0.652864531
Thioredoxin domain-containing protein 5	Q8NBS9	0.0035843	0.2885533	1.59440314	0.825564784
Prolargin	P51888	0.0033696	0.2270366	2.96971508	0.943620631
Dolichyl-diphosphooligosaccharide-protein glycosyltransferase subunit 2	P04844	0.0033509	0.0116242	1.53964014	1
Plastin-2	Q61233	0.0033047	0.3847723	1.99018513	0.598390619
Decorin	P07585	0.0032437	0.3171161	1.83686709	0.771824683
Protein disulfide-isomerase A4	P13667	0.0025061	0.2686129	1.69255519	0.871053227
Immunoglobulin heavy constant gamma 3	P01860	0.0024355	0.2726492	2.45801404	0.855543903
Heat shock-related 70 kDa protein 2	P54652	0.0023972	0.113302	1.71989491	0.999993783
Probable ATP-dependent RNA helicase DDX5	A5A6J2;P17844	0.00228	0.3255255	1.97935445	0.712840555
Coatomer subunit beta	O55029	0.0021076	0.2270366	3.10673893	0.946494099
Protein disulfide-isomerase A3	P30101	0.0017214	0.2000892	1.62917084	0.9859406
Immunoglobulin heavy constant gamma 4	P01861	0.0014507	0.3444506	2.15666663	0.672341363
Transitional endoplasmic reticulum ATPase	Q7ZU99	0.0012721	0.2270366	4.0405704	0.92861101
Periostin	Q62009	0.0012484	0.1683598	2.11026082	0.99758383
Keratin type II cytoskeletal 4	P19013	0.0011481	0.3943175	1.8453487	0.568928235
Dolichyl-diphosphooligosaccharide-protein glycosyltransferase subunit 1	P04843	0.0011056	0.2135866	1.63474264	0.975442197
Actin aortic smooth muscle	P62736;P63267	0.0008349	0.3255255	7.85237412	0.726979068
Keratin type II cytoskeletal 1	P04264;A5A6M6	0.0008055	0.1811616	2.45738148	0.995578171
Keratin type II cytoskeletal 6B	Q9Z331	0.0006659	0.1410083	6.63077012	0.999398198

Table 2. *The list of identified proteins (continued)*

Protein Name	Accession Number	P Value	Q Value	Fold Change	Power
Periostin	Q15063	0.0005452	0.2543735	1.57656593	0.884225394
Keratin type I cytoskeletal 19	P08727	0.0005163	0.1507498	2.40782814	0.998614781
Protein-glutamine gamma-glutamyltransferase E	Q08188	0.0004337	0.2479149	1.95355944	0.906833537
Endoplasmin	P14625	0.0002239	0.2543735	1.64650041	0.884267123
Keratin type I cytoskeletal 13	P13646;A5A6P3;O76009;O76011;Q9C075	0.0001589	0.113302	3.93747234	0.999978162
Keratin type II cytoskeletal 6A	P02538	0.000158	0.2543735	2.64170703	0.896233369
Apolipoprotein B-100	P04114	0.000000699	0.2689355	1.50061659	0.868712906
Derlin-2	Q9GZP9	0.0322501	0.3790223	1.59148063	0.609164362
Guanine nucleotide-binding protein G(I)/G(S)/G(T) subunit beta-1	P62873	0.0318179	0.3223091	1.65624766	0.743890989
Integrin-linked protein kinase	O55222;Q13418	0.0318036	0.3444506	19.6263433	0.646500435
Alpha-mannosidase 2	Q16706	0.0317961	0.2000892	2.24080842	0.985297612
ATP synthase subunit beta	P85446	0.0312786	0.2885533	5.80844931	0.821857339
High mobility group protein B1	P09429;P10103;P63159;B2RPK0	0.0311746	0.2471222	2.48853462	0.910609495
Immunoglobulin heavy variable 3-7	P01780;A0A0B4J1V1;P01762;P01763;A0A0B4J1X8;A0A0C4DH32;P01766	0.0311637	0.3171161	1.95019881	0.777037742
Torsin-1A-interacting protein 1	Q5JTV8	0.0305529	0.3847723	1.73495521	0.59826925
Ras-related protein Rab-3A	P20336	0.0300769	0.3255255	5.28473034	0.719461125
GTP-binding protein SAR1a	Q9NR31;Q9Y6B6	0.0280528	0.3223091	1.81775252	0.762300497

Figure 1. *Molecular function distribution of identified proteins by Panther Analysis*

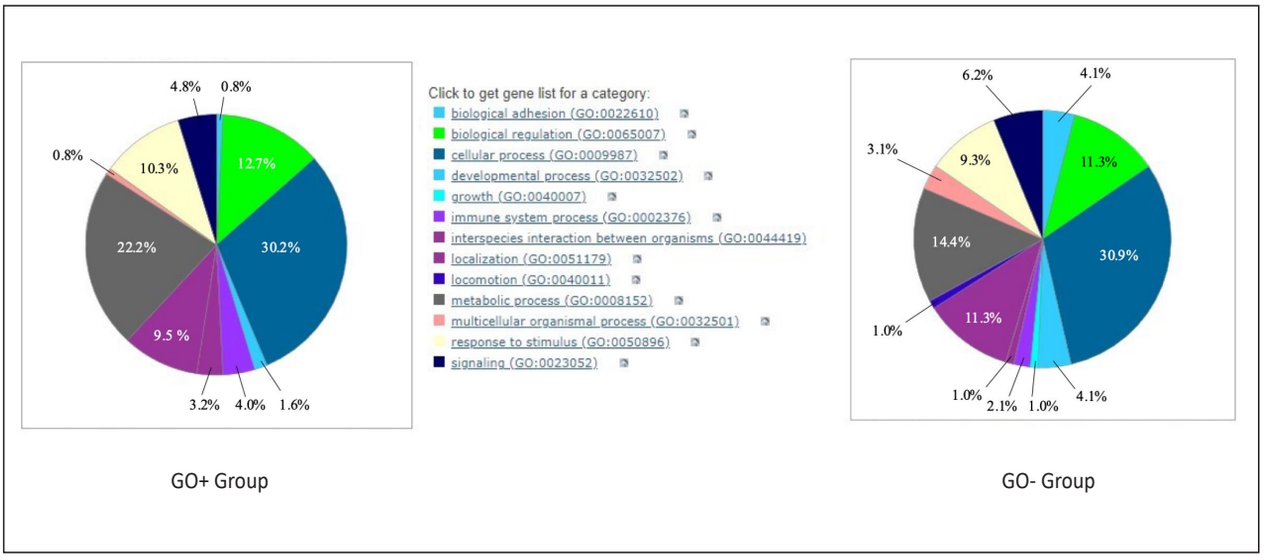

Figure 2. *Biological process distribution of proteins by Panther Analysis*

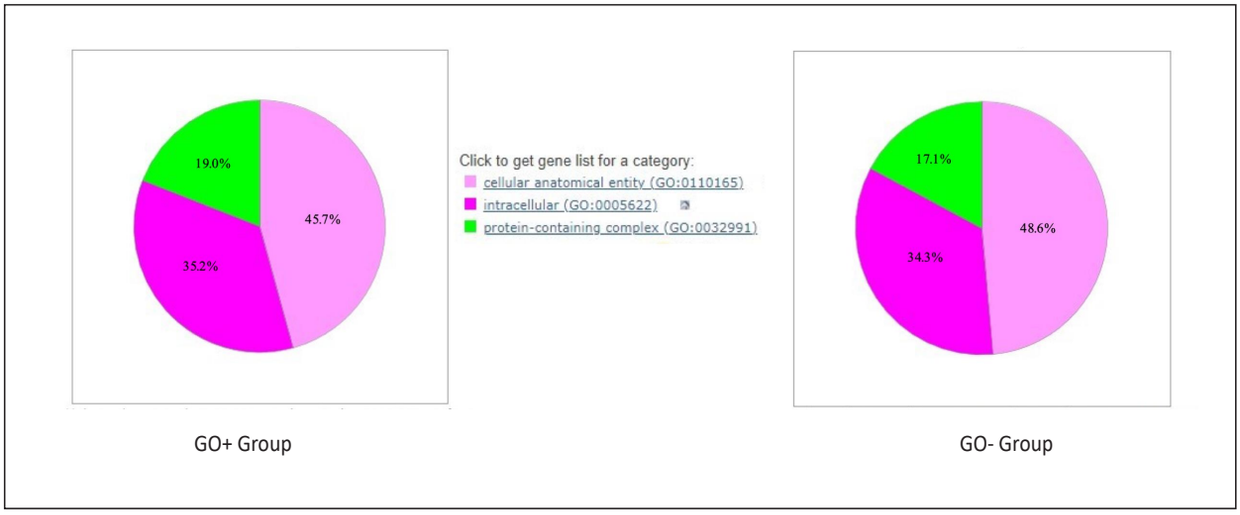

Figure 3. *Cellular component distribution of proteins by Panther Analysis*

4. DISCUSSION

DIGO is a well-known common side effect of systemically used drugs, including nifedipine. NIGO has been reported to possess the highest prevalance rate among other CCBs (24). Despite extensive in vivo and in vitro studies, the underlying pathological mechanism causing GO in affected individuals has not been fully defined as well as it is still unclear why some of the individuals using nifedipine develop GO while some others do not (25). In addition, the growth pattern of the same individual varies in different gingival regions. Recent studies have reported several associated factors such as genetic predisposition, decrease of cellular folate uptake, increased levels of certain cytokine and growth factors in overgrown gingiva (26, 27). Moreover, the severity degree of periodontal inflammation may play a role in the pathogenesis and onset of GO. Under nifedipine medication, GO may occur besides the existing periodontitis; also GO may be an initiative factor for periodontitis due to the poor oral hygiene and development of periodontal inflammation resulting with the increase in pocket depth. This cause-effect relation stil has not been illuminated (28).

Specifically, the proteome is defined as proteins that are produced in an organism under certain conditions, in a particular cell type or at a particular time. The main objective of proteomics is the rapid and quantitative characterization

of proteins. Proteomics provides biological information for many pathologies and is used to detect biomarkers of many tumours and inflammatory diseases, as well as to determine the expression of numerous proteins in cells (29).

The formation of wide and detailed expression profile database for NIGO is strongly requested and needed for better understanding its pathogenesis, discovering the potential biomarkers underlying the process and allowing an illumination for this unclear periodontal pathology. So far, the pathogenesis of NIGO has been studied in saliva, serum, gingival tissues and GCF with previously selected specific biomarkers, cytokines or genes (30, 31). However, a direct protein analysis of the overgrown gingival tissues is yet to be obtained to understand the underlying mechanism. The proteomics technique enables to uncover the biological substances and cell ingredients that may have a role in pathways leading to the clinical presentation of NIGO. Gingival tissue is the only biological material in which proteomics can offer the accurate molecular analysis.

In this cross-sectional study, the proteomic expression profiles related to overgrown gingival tissues were examined together with non-overgrown tissues of the same patients under systemic nifedipine treatment. The LC-MS/MS technique was chosen to evaluate and examine the protein content of the gingival tissues in detail, providing a basis for further studies on DIGO and NIGO, in particular.

Proteomics has been applied in medical sciences especially for the investigation of cancer and organ fibrosis (32, 33). The use of LC-MS/MS technique for proteomics has been performed in the field of periodontology recently. Tsuchida et al. (34) studied on GCF samples of healthy and chronic periodontitis individuals and identified 619 proteins of which several potential biomarkers for periodontal disease were included. McKnight et al. (35) identified 518 proteins of human gingival and periodontal ligament fibroblasts and compared with each other according to their functions. Yang et al. (36) examined the alveolar bone and surrounding soft tissue to further enlighten the regenerative process and healing. They revealed ECM associated proteins and showed soft and hard tissue interacted proteins during healing process (36). Reichenberg et al. (37) investigated the proteome map of human periodontal ligament fibrils obtained from extracted teeth and detected a total of 117 proteins with 9 different functions. The proteomic profiles of healthy and pathologic gingival pocket tissues were compared by Monari et al. (38) to analyze periodontal disease pathogenesis in more detail. They identified proteins associated with cell proliferation and apoptosis (38).

Currently, there is only one in vitro study in the literature on DIGO, in which proteomics was performed for gingival fibroblast cultures. Jung et al. (16) examined and quantified the proteins expressed by cultured gingival fibroblasts treated with cyclosporin-A at a concentration of 10 µM for 48 hours, and reported 17 proteins associated with cell proliferation.

In our study, proteomics was applied to analyze and compare the protein content of overgrown and non-overgrown gingival tissues of same patients under systemic nifedipine treatment aiming to recognize differently expressed proteins. So far, highly sensitive gel free LC-MS/MS approaches have not been performed on gingival tissues intending on research of NIGO.

The proteins identified in higher quantities in the GO+ group were found to be mainly associated with cell proliferation, growth and development. Among those, protein kinases are enzymes that regulate the biological activity of proteins (39). Pyruvate dehydrogenase kinase isozyme which is upregulated in GO+ group, has the protein kinase activity phosphorylating proteins resulting in enzyme activity and location changes. Pyruvate dehydrogenase kinase is crucial for maintaining energy homeostasis under certain conditions of overfeeding. Moreover, inappropriate suppression of this enyzme activity may promote the development of metabolic diseases. It controls the conversion of pyruvate, coenzyme A (CoA) and nicotinamide adenine dinucleotide (NAD) to acetyl-CoA, NAD + hydrogen (NADH) and CO_2, thus linking fatty acid metabolism, glucose metabolism and tricarboxylic acid cycle each other (40). Pyruvate dehydrogenase kinase, a mitochondrial enzyme, is activated in various forms of cancer, resulting in the selective inhibition of pyruvate dehydrogenase (41). Cell proliferation and prevention of the cell from apoptosis are the main roles of this enzyme that should be given attention to and may be correlated with overgrown gingival tissues. Macrophage migration inhibitory factor, striatin, myeloid-derived growth factor and thioredoxin domain containing protein are associated with fibroblast proliferation, growth factor mediated cell survival, tissue growth, tumor development and angiogenesis which were found to be upregulated in the GO+ group. Such proteins have been studied continously in a number of cancer and metabolic disease researches as their role in tissue growth and cell proliferation is remarkable (42). Therefore, connection of the above mentioned proteins with GO mechanism should be further examined. Derlin accounts for cell signaling and protein binding activity and regulates indirectly the insulin-like growth factor receptor signaling pathway. Insulin-like growth factor was reported to be related with GO (43). Derlin protein was also analyzed in organ fibrosis and cancer and was reported to have indirect interaction with renal fibrosis and lung adenocarcinoma (44). Also, fibrosis of gingival tissues occurs as a clinical presentation of DIGO. Annexin plays a role in wound healing and inflammatory response. As a result of the imbalance of the injury-repair response, the number of fibroblasts remains elevated leading to collagen deposition (45). Besides this important function, Annexin acts as a responder to drugs in organisms (46). This function appears to be spectacular indicator for overgrown tissues under systemic nifedipine use. Jung et al. (16) reported downregulated levels of Annexin in cyclosporin-A treated gingival fibroblasts in vitro. This finding contradicts with our result in which the GO+ group showed high levels of Annexin protein. Peroxiredoxin has a

role in response to oxidative stress which protects the cell against damages of reactive oxygen species, inhibiton of cell apoptosis, organization of the ECM and management of cell proliferation (47). These activities indicate that peroxiredoxin may account for NIGO, hence significantly increased level of peroxiredoxin was determined in the GO+ group. Parallel to our finding, Jung et al. (16) reported elevated levels of peroxiredoxins in cyclosporin-A treated gingival fibroblasts.

Proteins related with cell apoptosis and growth regulation were detected higher in the GO- group. One of them was integrin-linked protein kinase, that takes place in growth factor signaling pathway and tumor necrosis factor-mediated signaling pathway (48). The initiation of tumor necrosis factor pathway results in downregulation of cellular processes such as transcription. Thus, this function may explain the increased level of this protein in the GO- group. CDKN2A-interacting protein has a role in signaling pathways involved in cell growth and apoptosis and regulates these processes in either up or down regulatory ways (49). Programmed cell death protein is responsible for down-regulation of cell proliferation, up-regulation of apoptosis and inflammatory response (50). Since this protein appeared to be upregulated in the GO- group, it warrants further research in the pathogenesis of NIGO.

5. CONCLUSION

The defined proteins expressed at different levels in both groups may contribute to the pathogenesis of NIGO. Further quantitative confirmation of these proteins by Western Blot is needed to understand their regulatory roles. Our study is the first which compares the proteomic profile of over-grown (GO+) and non-overgrown (GO-) gingival regions of the same individuals under systemic nifedipine treatment. In conclusion, although limited number of proteins were discovered, the obtained data support that up-regulated or down-regulated proteins may play roles in NIGO pathogenesis. The formation of a strong and detailed proteomic expression profile knowledge for NIGO would be valuable to understand the pathogenesis and progression of this clinical phenomenon and to establish new therapeutic strategies.

Acknowledgement

This study was supported financially by Marmara University Scientific Research Project Department (project support #: SAG-C-DRP-110.718.0437).

Conflicts of interest

No potential conflict of interest was reported by any of the authors in this study.

REFERENCES

[1] Seymour RA, Ellis JS, Thomason JM. Risk factors for drug-induced gingival overgrowth. J Clin Periodontol 2000;27(4):217-223.

[2] Hassell TM, Hefti AF. Drug-induced gingival overgrowth: old problem, new problem. Crit Rev Oral Biol Med 1991;2(1):103-137.

[3] Newman T, Klokkevold, Carranza. Newman and Carranza's Clinical Periodontology. 2019;13:19-287.

[4] Seymour RA. Calcium channel blockers and gingival overgrowth. Br Dent J 1991;170(10):376-379.

[5] Barak S, Engelberg IS, Hiss J. Gingival hyperplasia caused by nifedipine. Histopathologic findings. J Periodontol 1987;58(9):639-642.

[6] Steele RM, Schuna AA, Schreiber RT. Calcium antagonist-induced gingival hyperplasia. Ann Intern Med 1994;120(8):663-664.

[7] Miller CS, Damm DD. Incidence of verapamil-induced gingival hyperplasia in a dental population. J Periodontol 1992;63(5):453-456.

[8] Gelfand EW, Cheung RK, Grinstein S, Mills GB. Characterization of the role for calcium influx in mitogen-induced triggering of human T cells. Identification of calcium-dependent and calcium-independent signals. Eur J Immunol 1986;16(8):907-912.

[9] Sooriyamoorthy M, Gower DB, Eley BM. Androgen metabolism in gingival hyperplasia induced by nifedipine and cyclosporin. J Periodontal Res 1990;25(1):25-30.

[10] Saito K, Mori S, Iwakura M, Sakamoto S. Immunohistochemical localization of transforming growth factor beta, basic fibroblast growth factor and heparan sulphate glycosaminoglycan in gingival hyperplasia induced by nifedipine and phenytoin. J Periodontal Res 1996;31(8):545-555.

[11] Balaji A, Balaji TM, Rao SR. Angiotensin II levels in gingival tissues from healthy individuals, patients with nifedipine induced gingival overgrowth and non nesponders on nifedipine. J Clin Diagn Res 2015;9(8):Zc92-94.

[12] Ghallab NA. Diagnostic potential and future directions of biomarkers in gingival crevicular fluid and saliva of periodontal diseases: Review of the current evidence. Arch Oral Biol 2018;87:115-124.

[13] Jágr M, Eckhardt A, Pataridis S, Broukal Z, Dušková J, Mikšík I. Proteomics of human teeth and saliva. Physiol Res 2014;63(Suppl 1):S141-154.

[14] Mohd Nasri FA, Zainal Ariffin SH, Karsani SA, Megat Abdul Wahab R. Label-free quantitative proteomic analysis of gingival crevicular fluid to identify potential early markers for root resorption. BMC Oral Health 2020;20(1):256.

[15] Fleissig Y, Reichenberg E, Redlich M, Zaks B, Deutsch O, Aframian DJ, Palmon A. Comparative proteomic analysis of human oral fluids according to gender and age. Oral Dis 2010;16(8):831-838.

[16] Jung JY, Kang GC, Jeong YJ, Kim SH, Kwak YG, Kim WJ. Proteomic Analysis in Cyclosporin A-Induced Overgrowth of Human Gingival Fibroblasts. Biological and Pharmaceutical Bulletin 2009;32(8):1480-1485.

[17] Silness J, Loe H. Periodontal disease in pregnancy. II. Correlation between oral hygiene and periodontal condition. Acta Odontol Scand 1964;22:121-135.

[18] Loe H, Silness J. Periodontal disease in pregnancy. I. Prevalence and severity. Acta Odontol Scand 1963;21:533-551.

[19] Ellis JS, Seymour RA, Robertson P, Butler TJ, Thomason JM. Photographic scoring of gingival overgrowth. J Clin Periodontol 2001;28(1):81-85.

[20] He F. Bradford Protein Assay. Bio-protocol 2011;1(6):e45.

[21] Wiśniewski JR, Zougman A, Nagaraj N, Mann M. Universal sample preparation method for proteome analysis. Nat Methods 2009;6(5):359-362.

[22] Consortium TU. UniProt: the universal protein knowledgebase in 2021. Nucleic Acids Res 2020;49(D1):D480-D489.

[23] Mi H, Ebert D, Muruganujan A, Mills C, Albou L-P, Mushayamaha T, Thomas PD. PANTHER version 16: a revised family classification, tree-based classification tool, enhancer regions and extensive API. Nucleic Acids Res 2020;49(D1):D394-D403.

[24] Hallmon WW, Rossmann JA. The role of drugs in the pathogenesis of gingival overgrowth. A collective review of current concepts. Periodontol 2000 1999;21:176-196.

[25] Kose KN, Yilmaz S, Noyan U, Kuru B, Yildirim HS, Agrali OB, Ozener HO, Kuru L. The gingival crevicular fluid levels of growth factors in patients with amlodipine-induced gingival overgrowth: A pilot study. Niger J Clin Pract 2020;23(4):561-567.

[26] Kuru L, Yilmaz S, Kuru B, Kose KN, Noyan U. Expression of growth factors in the gingival crevice fluid of patients with phenytoin-induced gingival enlargement. Arch Oral Biol 2004;49(11):945-950.

[27] Uzel MI, Kantarci A, Hong HH, Uygur C, Sheff MC, Firatli E, Trackman PC. Connective tissue growth factor in drug-induced gingival overgrowth. J Periodontol 2001;72(7):921-931.

[28] Tavassoli S, Yamalik N, Caglayan F, Caglayan G, Eratalay K. The clinical effects of nifedipine on periodontal status. J Periodontol 1998;69(2):108-112.

[29] Ogita M, Tsuchida S, Aoki A, Satoh M, Kado S, Sawabe M, Nanbara H, Kobayashi H, Takeuchi Y, Mizutani K, Sasaki Y, Nomura F, Izumi Y. Increased cell proliferation and differential protein expression induced by low-level Er:YAG laser irradiation in human gingival fibroblasts: proteomic analysis. Lasers Med Sci 2015;30(7):1855-166.

[30] George A, George SP, John S, George N, Joe S, Mathew R. Changes in inflammatory markers in bacterial – and nifedipine-induced gingival inflammation. J Int Oral Health 2015;7(Suppl 2):64-67.

[31] Ju Y, Huang L, Wang S, Zhao S. Transcriptional analysis reveals key genes in the pathogenesis of nifedipine-induced gingival overgrowth. Anal Cell Pathol (Amst) 2020;2020:6128341.

[32] Gong Q, Zhang X, Liang A, Huang S, Tian G, Yuan M, Ke Q, Cai Y, Yan B, Wang J, Wang J. Proteomic screening of potential N-glycoprotein biomarkers for colorectal cancer by TMT labeling combined with LC-MS/MS. Clin Chim Acta 2021;521:122-130.

[33] Xu L, Tan B, Huang D, Yuan M, Li T, Wu M, Ye C. Remdesivir inhibits tubulointerstitial fibrosis in obstructed kidneys. Front Pharmacol 2021;12:626510.

[34] Tsuchida S, Satoh M, Kawashima Y, Sogawa K, Kado S, Sawai S, Nishimura M, Ogita M, Takeuchi Y, Kobyashi H, Aoki A, Kodera Y, Matsushita K, Izumi Y, Nomura F. Application of quantitative proteomic analysis using tandem mass tags for discovery and identification of novel biomarkers in periodontal disease. Proteomics 2013;13(15):2339-2350.

[35] McKnight H, Kelsey WP, Hooper DA, Hart TC, Mariotti A. Proteomic analyses of human gingival and periodontal ligament fibroblasts. J Periodontol 2014;85(6):810-818.

[36] Yang HY, Kwon J, Kook MS, Kang SS, Kim SE, Sohn S, Jung S, Kwon SO, Kim HS, Lee JH, Lee TH. Proteomic analysis of gingival tissue and alveolar bone during alveolar bone healing. Mol Cell Proteomics 2013;12(10):2674-2688.

[37] Reichenberg E, Redlich M, Cancemi P, Zaks B, Pitaru S, Fontana S, Pucci-Minafra I, Palmon A. Proteomic analysis of protein components in periodontal ligament fibroblasts. J Periodontol 2005;76(10):1645-1653.

[38] Monari E, Cuoghi A, Bellei E, Bergamini S, Lucchi A, Tomasi A, Cortellini P, Zaffe D, Bertoldi C. Analysis of protein expression in periodontal pocket tissue: a preliminary study. Proteome Sci 2015;13:33.

[39] Tuganova A, Boulatnikov I, Popov KM. Interaction between the individual isoenzymes of pyruvate dehydrogenase kinase and the inner lipoyl-bearing domain of transacetylase component of pyruvate dehydrogenase complex. Biochem J 2002;366(Pt 1):129-136.

[40] Zhang S, Hulver MW, McMillan RP, Cline MA, Gilbert ER. The pivotal role of pyruvate dehydrogenase kinases in metabolic flexibility. Nutr Metab (Lond) 2014;11(1):10.

[41] Sutendra G, Michelakis ED. Pyruvate dehydrogenase kinase as a novel therapeutic target in oncology. Front Oncol 2013;3:38.

[42] Sumaiya K, Langford D, Natarajaseenivasan K, Shanmughapriya S. Macrophage migration inhibitory factor (MIF): A multifaceted cytokine regulated by genetic and physiological strategies. Pharmacol Ther 2021:108024.

[43] Subramani T, Rathnavelu V, Alitheen NB. The possible potential therapeutic targets for drug induced gingival overgrowth. Mediators Inflamm 2013;2013:639468.

[44] Zhang F, Zhou X, Zou H, Liu L, Li X, Ruan Y, Xie Y, Shi M, Xiao Y, Wang Y, Zhou Y, Wu Y, Guo B. SAA1 is transcriptionally activated by STAT3 and accelerates renal interstitial fibrosis by inducing endoplasmic reticulum stress. Exp Cell Res 2021;408(1):112856.

[45] Lim HI, Hajjar KA. Annexin A2 in fibrinolysis, inflammation and fibrosis. Int J Mol Sci 2021;22(13).

[46] Schuliga M, Jaffar J, Berhan A, Langenbach S, Harris T, Waters D, Lee PVS, Grainge C, Westall G, Knight D, Stewart AG. Annexin A2 contributes to lung injury and fibrosis by augmenting factor Xa fibrogenic activity. Am J Physiol Lung Cell Mol Physiol 2017;312(5):L772-l82.

[47] Hofmann B, Hecht HJ, Flohé L. Peroxiredoxins. Biol Chem 2002;383(3-4):347-64.

[48] Yuan D, Zhao Y, Wang Y, Che J, Tan W, Jin Y, Wang F, Li P, Fu S, Liu Q, Zhu W. Effect of integrin-linked kinase gene silencing on microRNA expression in ovarian cancer. Mol Med Rep 2017;16(5):7267-7276.

[49] Potrony M, Haddad TS, Tell-Martí G, Gimenez-Xavier P, Leon C, Pevida M, Mateu J, Badenas C, Carrera C, Malvehy J, Aguilera P, Llames S, Escámez MJ, Puig-Butillé JA, Del Río M, Puig S. DNA repair and immune response pathways are deregulated in melanocyte-keratinocyte co-cultures derived from the healthy skin of familial melanoma patients. Front Med (Lausanne) 2021;8:692341.

[50] Yamane H, Isozaki H, Takeyama M, Ochi N, Kudo K, Honda Y, Yamagishi T, Kubo T, Kiura K, Takigawa N. Programmed cell death protein 1 and programmed death-ligand 1 are expressed on the surface of some small-cell lung cancer lines. Am J Cancer Res 2015;5(4):1553-1557.

How to cite this article: Yetis E, Yarat A, Eroglu O, Ozturk Ozener H, Kuru L. Proteomic Analysis in Nifedipine Induced Gingival Overgrowth: A Pilot Study. Clin Exp Health Sci 2022; 12: 1013-1024. DOI: 10.33808/clinexphealthsci.1050418